THE EFFECT OF RESIDUAL CALCIUM IN DECALCIFIED FREEZE-DRIED BONE ALLOGRAFT IN A CRITICAL-SIZED DEFECT IN THE *RATTUS NORVEGICUS* CALVARIUM

James W. Turonis, DDS, MS
James C. McPherson III, PhD
Michael F. Cuenin, DMD
Steven D. Hokett, DDS
Mark E. Peacock, DDS, MS
Mohamed Sharawy, BdS, PhD

KEY WORDS

Bone regeneration
Demineralized freeze-dried bone allograft
Freeze-dried bone allograft
Rat
Calvaria
Calcium
Polytetrafluoroethylene

James W. Turonis, DDS, MS, Michael F. Cuenin, DMD, *and* ***Mark E. Peacock, DDS, MS,*** *are currently stationed with the US Army Dental Corps in Germany.*

James C. McPherson III, PhD, *is from the Department of Clinical Investigation at Eisenhower Army Medical Center in Fort Gordon, Ga.*

Steven D. Hokett, DDS, *is currently in the private practice of Periodontics in Vancouver, Wash. Address correspondence to Dr Steven D. Hokett, 18014 NE 85th Way, Vancouver, WA 89682 (e-mail: hoketts@ohsu.edu).*

Mohamed Sharawy, BdS, PhD, *is from the Medical College of Georgia in the Department of Oral Biology in Augusta, Ga.*

Demineralized freeze-dried bone allograft (DFDBA), a widely used graft material in periodontal regenerative procedures, is processed with hydrochloric acid in the attempt to expose proteins located within the bone matrixes that are capable of inducing new bone formation. However, the degree of DFDBA demineralization varies between tissue banks, which may have an effect on clinical regeneration. This study uses the critical-sized defect (CSD) model to evaluate the wound-healing response to the residual calcium of donor bone. If the percentage of residual calcium in a graft were demonstrated to significantly enhance wound healing, then periodontal patients may benefit from further standardization of human-allograft processing. Sixty adult, male, Harlan Sprague-Dawley rats (*Rattus norvegicus*) were randomly and equally divided into 4 test groups (ie, DFDBA at 1%, 2%, and 3% to 6% residual calcium levels and FDBA at 23% residual calcium) and a control group (no allograft). An 8-mm-diameter craniotomy was made in the rat calvarium, and polytetrafluoroethylene membranes with pore sizes of 0.50 μm were placed intracranially and ectocranially. Treatment materials were carefully placed into the CSD with a new sterilized dental amalgam carrier. Tetracycline hydrochloride was injected intraperitoneally for labeling new bone growth, and animals were euthanized 12 weeks postsurgery. As a result, histomorphometric bone fill at 12 weeks showed a statistically significant increase in the 2% DFDBA group as compared to all other groups. The authors conclude that a 2% residual calcium level in human DFDBA appears to significantly ($P \leq .05$) enhance osseous wound healing in the rat calvarium.

Introduction

Regenerative periodontal therapy currently makes use of bone substitutes in the form of autografts, allografts, alloplasts, and occlusive membranes to enhance clinical results.[1–3] The volume of potential host donor bone available to graft severe osseous defects is often inadequate, and procedures required for harvesting may produce significant morbidity. Commercial allograft materials such as demineralized freeze-dried bone allograft (DFDBA) and freeze-dried bone allograft (FDBA) are currently in widespread clinical use. Allograft demineralization exposes bone morphogenetic proteins, which have been shown to stimulate new bone formation. However, it has been proposed that a specific level of residual calcium in the DFDBA matrix is also necessary to stimulate osteoblasts to form bone.[4] Research has shown that the level of residual calcium in the DFDBA matrix should be 2% for optimal osteoinductive potential in male athymic mice.[4,5] Another research group demonstrated that porcine osteoclasts show significantly more resorptive activity as measured on calcium phosphate–coated discs in the presence of 2.41% residual calcium in DFDBA than in other DFDBA residual-calcium levels.[6] The significance of this finding is that osteoclast activation may accelerate allograft replacement and subsequent osteogenesis. The rat critical-sized defect (CSD) model in the craniomandibulofacial region permits an in vivo evaluation of cellular response characterization, biodegradation, and biocompatibility of these osseous graft materials prior to testing in higher phylogenetic species.[7]

Occlusive periodontal membranes are an integral component in periodontal-regeneration procedures because they provide a physical barrier to the rapidly migrating epithelial and connective tissue cells and, thus, permit the slower-migrating mesenchymal cells from the surrounding bone and bone marrow to selectively repopulate the defect.[8,9] This study uses the CSD model with polytetrafluoroethylene (PTFE) membranes and human allograft to evaluate the wound-healing response to small changes in the percentage of calcium in the rat calvarium. If the percentage of residual calcium within a human allograft were demonstrated to significantly enhance wound healing, then periodontal patients may benefit from further standardization of human allograft processing.

Materials and Methods

Sixty adult, male, Harlan Sprague-Dawley rats (*Rattus norvegicus*), approximately 92 to 105 days old and ranging in weight from 325 g to 375 g were randomly and equally divided into 4 test groups (DFDBA at 1%, 2%, and 3% to 6% residual calcium levels and FDBA at 23% residual calcium), and a control group (no allograft). The Institutional Care and Animal Use Committee at Dwight David Eisenhower Army Medical Center in Fort Gordon, Ga, approved and governed this research protocol (DDEAMC 98-09).

Surgical procedure

Animals were intramuscularly anesthetized with a cocktail of Ketamine HCL, 100 mg/mL (150 mg total); Xylazine HCl, 20 mg/mL (30 mg total); and Acepromazine 10 mg/mL (5 mg total) and subsequently maintained on isoflurane 0.25% to 0.5% with oxygen 1 L/min. Under sterile conditions, an 8-mm-diameter craniotomy was made with a trephine bur under copious saline irrigation, and a PTFE membrane (Millipore Corporation, Bedford, Mass) with a pore size of 0.50 μm was placed extradurally (intracranial). Each of the corresponding experimental groups used a graft material with a particle size that ranged from 250 μm to 710 μm (LifeNet Transplant Services, Virginia Beach, Va). Seven vials of graft material from each group were mixed together to eliminate the variability of donor age and osteoinductive activity. The treatment materials appropriate to each study group were carefully placed into the CSD with a new sterilized dental amalgam carrier. The defect was covered on the extracranial aspect by second membrane extending 2 mm to 3 mm beyond the CSD surface. The periosteum was then repositioned and sutured, and the overlying skin was also repositioned and sutured. All animals were monitored for any signs of postsurgical pain or distress, and analgesics were not required.

Histology of demineralized specimens

All animals were euthanized and decapitated at 12 weeks postsurgery. Specimens were carefully sectioned sagittally to yield 2 equal samples; one sample was demineralized for histologic evaluation to determine the amount of fill across the coronal plane. Multiple, 5- to 6-μm sections were cut from each sample, and representative sections were stained with hematoxylin and eosin (H&E). The second sample was paraffin-embedded undemineralized for

fluorescence and histomorphometric evaluation.

Histomorphometry of undemineralized specimens

The undemineralized slides were embedded in methylmethacrylate, sectioned to a thickness of 100 μm, and stained using a modified Masson's trichrome stain. The sections were then captured with a color video camera attached to a microscope (original magnification ×125) (Sony, Japan) on a computer capture board and imaged with Image Pro-Plus software (Media Cybernetics, Silver Spring, Md). Each 9-mm region of interest (ROI) was captured in 1/5 or 1/4 sections due to the limitations of the 2× lens and analyzed for percent area of membranes, bone, DFDBA or FDBA, and connective tissue. The sections were then combined to give the percent total area of the membranes, bone, DFDBA or FDBA, and connective tissue for each ROI.

Vital staining

Tetracycline hydrochloride (TCN) 20 mg/kg dissolved in 1-mL saline was injected intraperitoneally each 14th day, beginning at the time of surgery and up to the 12-week time of sacrifice in order to monitor new bone growth via fluorescent microscopy. The bone-formation rate from each representative sample was calculated by averaging 5 measurements from the densest part of each TCN band.

Densitometry

The superior aspect of the calvaria surrounding the 8-mm-diameter defect was radiographed using a mammography X-ray unit set at 22 kv and 200 msec with an M0 filter. Computer scanning of the images was done and subsequently used to evaluate the percent defect bone fill (ImagePC, National Institute of Health, Bethesda, Md). A standardized, 9-mm, circular ROI was placed on each digital image, and the mean percent bone fill within the ROI was determined.

Statistical analysis

One-way analysis of variance was applied to determine if there were any significant differences in the observation made (eg, connective tissue, bone fill) among the groups tested. The Student Newman-Keuls test was then utilized to compare the groups. A P value of $\leq .05$ was considered to be statistically significant (SAS Version 6.12, SAS Institute Cary, NC). The values presented are the means ± SEM.

Results

Histology

In both the control and experimental specimens there was evidence of new bone formation both within and outside the membranes. The bone appeared to be vital due to the presence of osteocytes within their respective lacunae (Figure 1). The preponderance of bone varied from specimen to specimen. The control group showed bone regeneration at the peripheral edge and on the dural and periosteal side of the membranes. This bone appeared to be vital, and osteoblasts could be seen in new haversian canals (Figure 1). In the experimental groups, remnants of bone particles either surrounded by connective tissue or incorporated within the bony matrix were observed (Figures 2 and 3). The selected photomicrographs of the 1% and 2% DFDBA groups indicated only a minimal amount of unincorporated residual bone particles. Most of the bone particles appeared to have been incorporated into the mass of newly forming bone, with new bone almost completely filling the defect. The 2% DFDBA group demonstrated an amalgamation of the decalcified bone particles (DBP) and new vital bone in the center of the defect, forming a linked ''bridge'' over the defect. The remaining experimental groups had many more unincorporated residual bone particles (Figures 4 and 5).

Histomorphometry

A representative section of 2% residual calcium-filled CSD can be seen in Figure 6, which was used for histomorphometric analysis. In the center of the defect, the amount of new bone can be appreciated. The area fraction (Aa) of regenerated bone within the defect was statistically compared among the various groups (the Aa represents a fraction of the total area). The results indicate that there was no statistical difference between the Aa of the 1% DFDBA, 3% to 6% DFDBA, and the control group. There was a statistically significant ($P \leq .05$) increase in vital bone percentage, with the 2% DFDBA compared to all other groups (Figure 7).

Densitometric analysis

Radiographic images representing the 5 treatment groups are seen in Figure 8. A greater amount of bone fill, based on radiodensity, is visually evident within the CSD of the 2% DFDBA group. The bone appears more dense and compact within this group. A 9-mm-circular zone was evaluated around the 8-mm CSD to ensure that the entire defect was incorporated for the densitometric calculations. The total area in the

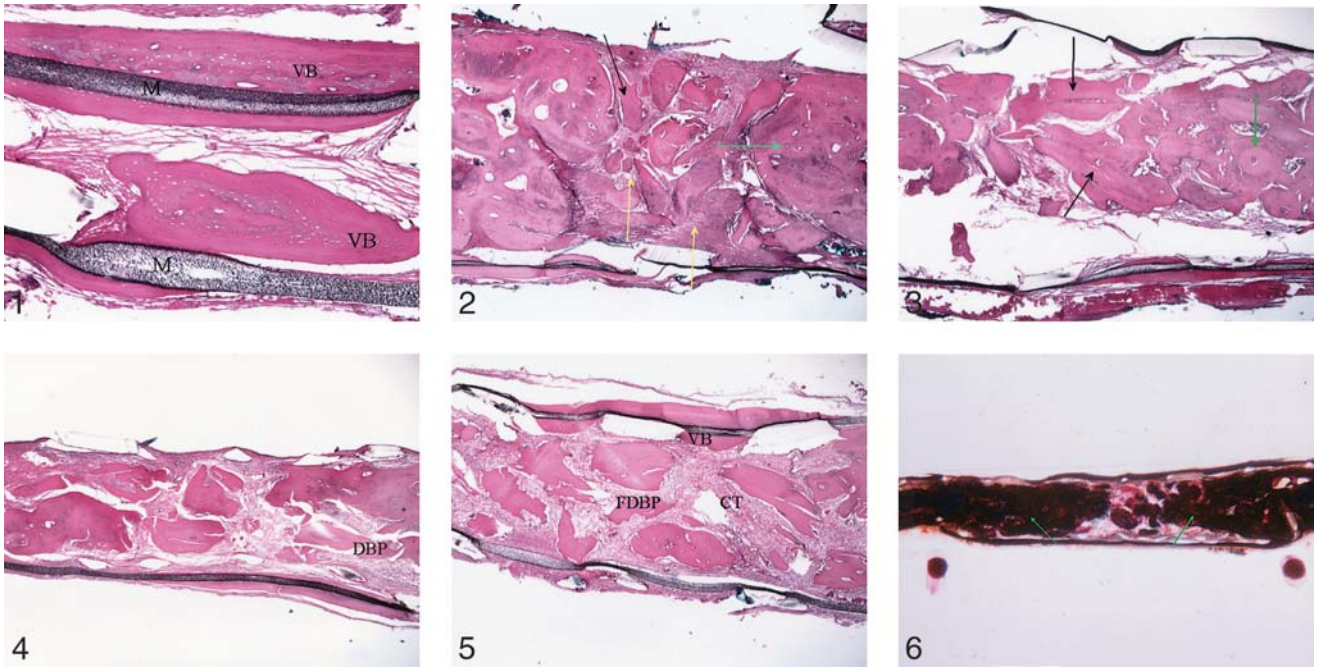

Figure 1. Decalcified hematoxylin and eosin histology of the critical-sized defect: control group. New vital bone (VB; original magnification ×125). High magnification of the central area of the defect showing a large bone island and bone on both sides of the membrane (M).

Figure 2. Decalcified hematoxylin and eosin histology of the critical-sized defect: 1% demineralized freeze-dried bone allograft (DFDBA). Central area of the defect (original magnification ×31.25). The center of the defect showing decalcified bone particles (DBPs; black arrow) surrounded by connective tissue (yellow arrows), the edges consist of solid bone with an amalgamation of DBPs and new bone (green arrow). Bone linking is not as evident as with 2% DFDBA (Figure 3).

Figure 3. Decalcified hematoxylin and eosin histology of the critical-sized defect (CSD): 2% demineralized freeze-dried bone allograft. Center of CSD (original magnification ×31.25). Center of defect showing an amalgamation of the decalcified bone particles and the new vital bone that is forming a linked bridge over the CSD. New haversian canals that indicate maturation (green arrow) and the linking of new vital bone and decalcified-bone particle can be appreciated (black arrows).

Figure 4. Decalcified hematoxylin and eosin histology of the critical-sized defect: 3% to 6% demineralized freeze-dried bone allograft (DFDBA). Central area of the defect (original magnification ×31.25). The center of the defect shows an abundance of connective tissue compared to the 2% DFDBA group. Minimal haversian systems are seen indicating lack of complete maturation.

Figure 5. Decalcified hematoxylin and eosin histology of the critical-sized defect (CSD): freeze-dried bone allograft. Central area of the CSD (original magnification ×31.25). Center of defect shows unresorbed freeze-dried bone particle (FDBP) surrounded by an abundance of connective tissue (CT). Minimal new bone formation is evident within the CSD.

Figure 6. Undecalcified Modified Masson's trichrome histology of the critical-sized defect 2% demineralized freeze-dried bone allograft group (original magnification ×12.50). Arrows indicate amalgamation of decalcified bone particle and new bone.

ROI was $A^T = \pi(4.5)^2$. At the given threshold of 128, the area of the most radiodense tissue was measured (A^B). The percent fill of the radiodense tissue was then determined with the formula $\%Fill = A^B/A^T \bullet 100$. There was no significant difference in the percent bone fill between any of the experimental groups. However, all experimental groups were statistically different from the control ($n = 30$; $P < .05$; see the Table).

Fluorescent microscopy

Generally, the new bone within the center of the CSDs appeared to be amorphous and disorganized under fluorescent microscopy for all groups. Figures 9 and 10 show selected views of the tetracycline staining around individual bone particles for the experimental groups (taken at the center of the defects) and at the edge of the calvaria in the control group. The bone formation rate (BFR) was calculated to range from 2.85 μm to 4.20 μm per day in all groups. The data obtained were consistent with previous studies. These data demonstrate that the allograft materials stimulate new bone formation at a rate that is similar to host bone.

Discussion

Results have shown that the percent bone fill across the 8-mm

defect was statistically greater ($P \leq .05$) for the 2% DFDBA as compared to the other groups (see the Table). Interestingly, the 1% DFDBA, 3% to 6% DFDBA, and control groups had similar bone fill that may be due to the incorporation of all new bone (both within and along the membranes outer surface) into the total area. However, the FDBA had statistically significant less bone fill ($P \leq .05$). The mineralized nature of the FDBA may have impeded the remodeling process, as Urist and Strates have pointed out, by limiting the exposure of the underlying bone morphogenic proteins (BMPs).[10] In another study, the mineralized bone powder used was completely resorbed by the third week without bony repair of the cranial defects, whereas the DBP was not resorbed but became amalgamated within the new bone and predictably produced healing of cranial defects.[11] In the present study, however, the FDBA did not resorb after 12 weeks and there was less bony fill of the cranial defect compared to the DFDBA groups. In contrast, the DFDBA groups did show statistically greater amounts of bone fill and had become amalgamated within the new bone.

A 2% residual calcium level in demineralized bone has previously been demonstrated as being the optimal concentration for the induction of new bone.[4] In this study, it was concluded that this level of residual calcium may facilitate the remineralization process to proceed unimpeded. A lower residual calcium level may be optimal for osteoclast resorption, which would then stimulate the surrounding osteoblasts to align on the existing bone particle surface. However, it has been shown that the appearance of osteoblasts precedes the appearance of osteoclasts in demineralized bone matrix (DBM)–induced osteogenesis.[12] This would be consistent with the ability of BMPs within the DBM to cause a phenotypic change of local mesenchymal cells into osteoblasts, which would then have the potential to regulate the production of osteoclasts.

Realistically, it is probably a combination of these and as yet other unknown interactions. It should be emphasized that residual calcium levels are only one piece of the puzzle. The demineralization process used by the tissue bank, the molecular and structural characteristics of the bone graft material, the interactions of endogenous and exogenous growth factors, the morphology of a given osseous defect, and the immunologic response of the patient to the graft material are among the many

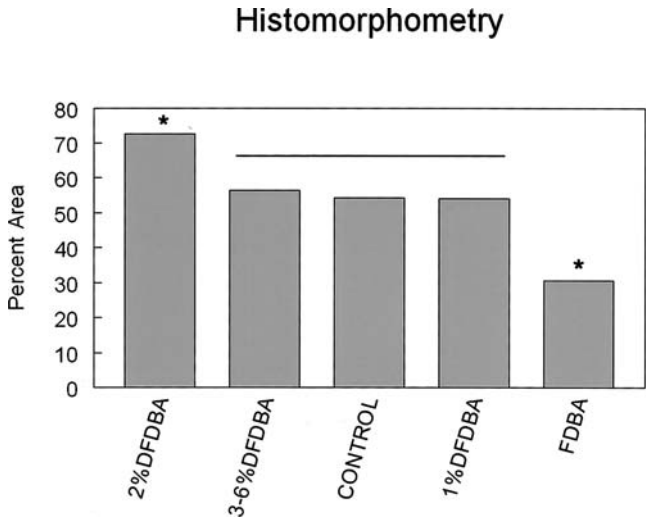

FIGURE 7. Mean percent total area of bone. The area fraction (Aa) of regenerated bone within the defects was statistically significant compared to the various groups. The dashed line indicates no statistical difference ($P \geq .05$) in the Aa between the 1% demineralized freeze-dried bone allograft (DFDBA), 3% to 6% DFDBA, and the control group, but the 2% DFDBA group showed statistically more vital bone compared to all other groups ($P \leq .05$). The height of the bar graph indicates the mean; *, statistical significance.

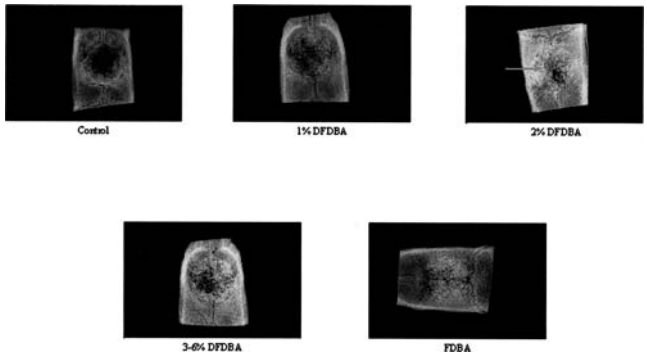

FIGURE 8. Densitometric view of all 5 treatment groups (1024 × 1024 dpi). Representative sections from each of the 5 treatment groups are shown. The arrow indicates a more uniform mass of new bone with the 2% demineralized freeze-dried bone allograft.

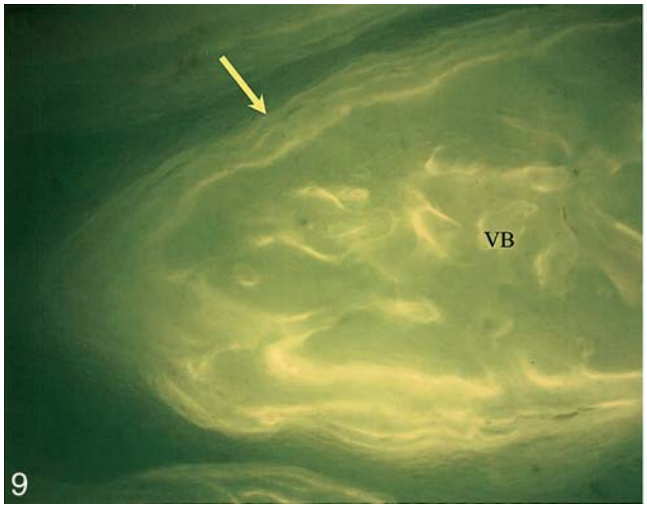

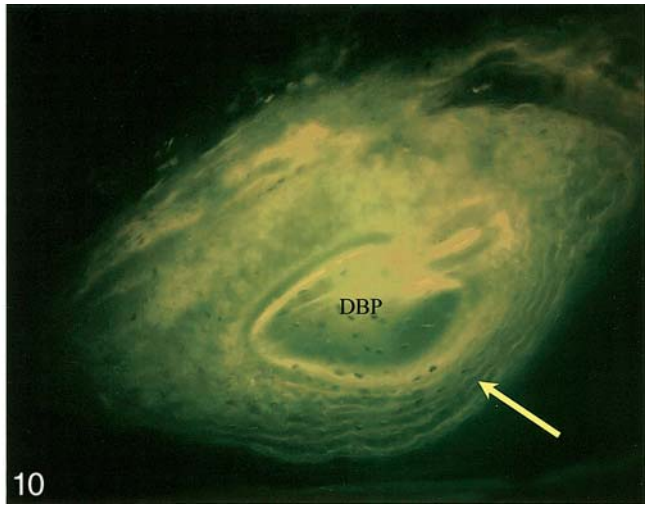

Figure 9. Tetracycline hydrochloride labeling of new bone: control group. Representative photomicrograph from the control group (original magnification ×100). The arrow indicates new bone formation near edge of defect (only 4 rings visible). (VB), vital bone.

Figure 10. Tetracycline hydrochloride labeling of new bone: 2% demineralized freeze-dried bone allograft (DFDBA) group. Two percent DFDBA particle at the center of defect (6 rings visible; original magnification ×100). The arrow shows the fourth administration of tetracycline hydrochloride at the 42-day time point. (DBP), decalcified bone particle.

factors involved in clinical bone-graft healing.

The densitometric analysis in this study was accomplished by calculating the percentage of bone filling an 8-mm craniotomy. The results indicated that there was statistical difference only between the experimental groups and the control. There was no statistical difference between the experimental groups themselves, even though the 2% DFDBA had a greater mean percent bone fill (see the Table). The difficulty with interpreting radiographs of DFDBA and FDBA is that the bone particles are radiopaque and, therefore, it makes it hard to discriminate calvarial bone from bone particles and new bone. Therefore, it was useful to correlate these results with histologic and vital staining techniques.

Fluorescent microscopy was accomplished by injecting tetracycline HCL (TCH) intraperitoneally at the time of surgery and at each succeeding 14-day period. The results of the fluorescent microscopy showed that the rate of bone formation across all 5 groups was similar. Throughout all the representative fluorescent slides, however, the TCH banding appeared to be diffuse. This diffuse labeling is most likely due to the large amount of woven or immature bone within these groups. This indicated that there was minimal mineralization, which occurred within the 12-week time period. If the study could have been extended over a 1-year time frame, the woven bone seen in these groups could reasonably be expected to have matured and become more mineralized as evidenced by an increase in lamellar organization and mineralization.

Table

Densitometric and histomorphic analyses*

Group	N	% Fill ± SEM	$P \leq .05$
Densitometric Analysis†			
FDBA	6	61.41 ± 9.8	No
1% DFDBA	6	53.04 ± 11	No
2% DFDBA	6	74.62 ± 6.9	No
3% to 6% DFDBA	6	45.01 ± 6.5	No
Control	6	21.42 ± 4.5	Yes
Histomorphic Analysis‡			
FDBA	6	30.55 ± 3.9	Yes
1% DFDBA	6	53.97 ± 3.55	No
2% DFDBA	6	72.50 ± 2.9	Yes
3% to 6% DFDBA	6	56.33 ± 4.59	No
Control	6	54.25 ± 3.22	No

*Densitometric analysis is the degree of fill of the bone defect. Histomorphic analysis is the percent area of bone fill within the defect.

†% Fill is the mean of the fractional amount of the total original defect area that is radiopaque. Complete filling would be 100%. SEM indicates standard error of the mean; FDBA, freeze-dried bone allograft; DFDBA, demineralized freeze-dried bone allograft.

‡% Fill is the mean total amount of bone seen in the defect. Complete filling would be 100%.

The BFR in various animal wound-healing models reveals varying rates of bone apposition. Measuring bone apposition rates in the femur of Sprague-Dawley rats, Tam and coworkers recorded mean values from 0.039 μm/h to 0.053 μm/h or 1.3 μm/d.[13] In a different study, Tam and Anderson recorded mean values from 0.038 μm/h to 0.040 μm/h in the same model.[14,15] In the present study, a bone formation rate of 2 μm/d to 4 μm/d was observed, which is substantially higher. Sharawy et al have shown that demineralized cranial bone powder may be more osteogeneic than demineralized bone powder from long bones and, thus, they have speculated that cranial bones may have more growth factors that must include a powerful angiogenic component.[16] This may account for the more rapid rate of bone formation rate observed in the present study.

The graft material used in this study is considered to be a xenograft because it was human bone that was placed into a rat. This may have had a negative impact on the total amount of bone fill. Previous studies have shown that xenogeneic bone grafts may be less effective than comparable allogeneic or autogeneous preparations.[17–19] However, other studies have shown that there is homology among bone-inductive proteins from human, monkey, bovine, and rat extracellular-bone matrices.[18,20] Positive results in rats have also been reported with xenogeneic porcine decalcified bone.[21–22] In a study by Hollinger and Kleinschmidt, the use of antigen-extracted allogeneic human bone in primates elicited an excellent response for new-bone production in the CSD.[7] In any case, the material used in the present study stimulated new-bone formation that was quantifiable despite the possible negative effects of its xenogenicity.

The H&E- and Modified Masson's Trichrome–stained sections showed an amalgamation of new and grafted bone. No evidence of inflammation or giant cell formation could be seen in any of the specimens. Further studies are needed to verify these results and, if the percentage of calcium is demonstrated to significantly enhance wound healing, then the techniques used to process human allograft may need further investigation.

Acknowledgments

The authors acknowledge the contributions of the members of the staff of Dr Mohamed Sharawy at the Medical College of Georgia for their extensive contributions to this research project. This study is in partial fulfillment of the Master of Science degree. The opinions expressed are not necessarily those of the US Army or the Department of Defense. This study was partially funded by the Southern Academy of Periodontology.

Note

The opinions expressed in this article are exclusively those of the authors and are not necessarily those of the US Army Dental Corps or the Department of the Army.

References

1. Brunsvold MA, Mellonig JT. Bone grafts and periodontal regeneration. *Periodontol 2000.* 1993;1:80–91.

2. Mellonig JT, Bowers GM. Regenerating bone in clinical periodontics. *J Am Dent Assoc.* 1990;121:497–502.

3. Mellonig JT. Freeze-dried bone allografts in periodontal reconstructive surgery. *Dent Clin North Am.* 1991;35:505–520.

4. Zhang M, Powers RM Jr, Wolfinbarger L Jr. Effect(s) of the demineralization process on the osteoinductivity of demineralized bone matrix. *J Periodontol.* 1997;68:1085–1092.

5. Zhang M, Powers RM Jr, Wolfinbarger L Jr. A quantitative assessment of osteoinductivity of human demineralized bone matrix. *J Periodontol.* 1997; 68:1076–1084.

6. Herold RW, Pashley DH, Cuenin MF, et al. The effects of varying degrees of allograft decalcification on cultured porcine osteoclasts cells. *J Periodontol.* 2002; 73:213–219.

7. Hollinger JO, Kleinschmidt JC. The critical size defect as an experimental model to test bone repair materials. *J Craniofac Surg.* 1990;1:60–68.

8. Caton JG, Polson AM, Prato GP, Bartolucci EG, Clauser C. Healing after application of tissue-adhesive material to denuded and citric acid-treated root surfaces. *J Periodontol.* 1986;57:385–390.

9. Melcher AH. On the repair potential of periodontal tissues. *J Periodontol.* 1976;47:256–260.

10. Urist MR, Strates BS. Bone formation in implants of partially and wholly demineralized bone matrix: including observations on acetone-fixed intra and extracellular proteins. *Clinical Orthop Relat Res.* 1970;71:271–278.

11. Glowacki J, Altobelli D, Mulliken JB. Fate of mineralized and demineralized osseous implants in cranial defects. *Calcif Tissue Int.* 1981;33:71–76.

12. Bagi CM, Miller SC. Ultrastructure, tartrate-resistant acid phosphatase activity and calcitonin responsiveness of osteoclasts at sites of demineralized bone matrix implant-induced osteogenesis. *Clin Orthop.* 1991;269:257–265.

13. Tam CS, Harrison JE, Reed R, Cruickshank B. Bone apposition rate as an index of bone metabolism. *Metabolism.* 1978;27:143–150.

14. Tam CS, Anderson W. Tetracycline labeling of bone in vivo. *Calcif Tissue Int.* 1980;30:121–125.

15. Francis PO, McPherson JC, Cuenin MF, et al. Evaluation of a novel alloplast for osseous regeneration in the rat calvarial model. *J Periodontol.* 2003;74:1023–1031.

16. Sharawy M, El- Shazly D, Um IW, Sohn J, Larke V, Pennington C. Study of interface bone induced between allogeneic cranial bone blocks used as onlay grafts in rabbits and rhesus monkeys. *Proceedings of the International*

Symposium on Formation and Repair of Mineralized Extracellular Matrix. Hong Kong; 1996.

17. Marinak KW, Mellonig JT, Towle HJ. The osteogenic potential of two human demineralized bone preparations using a xenogeneic model. *J Periodontol.* 1989;60:12–18.

18. Sampath TK, Reddi AH. Homology of bone-inductive proteins from human, monkey, bovine, and rat extracellular matrix. *Proc Natl Acad Sci U S A.* 1983;80:6591–6595.

19. Urist MR, Dowell TA. The newly deposited mineral in cartilage and bone matrix. *Clin Orthop.* 1967;50:291–308.

20. Sampath TK, Reddi AH. Dissociative extraction and reconstitution of extracellular matrix components involved in local bone differentiation. *Proc Natl Acad Sci U S A.* 1981;78:7599–7603.

21. Thielemann F, Veihelmann D, Schmidt K. The induction of new bone formation after transplantation [in German]. *Arch Orthop Trauma Surg.* 1978;91:3–9.

22. Thielemann FW, Schmidt K, Koslowski L. Osteoinduction, part II: purification of the osteoinductive activities of bone matrix. *Arch Orthop Trauma Surg.* 1982;100:73–78.